HAL
open science

Ion diamagnetic effects in gyrofluid collisionless magnetic reconnection

Daniela Grasso, François Waelbroeck, Emanuele Tassi

To cite this version:

Daniela Grasso, François Waelbroeck, Emanuele Tassi. Ion diamagnetic effects in gyrofluid collisionless magnetic reconnection. Journal of Physics: Conference Series, 2012, pp.012008. hal-00798203

HAL Id: hal-00798203

https://hal.science/hal-00798203v1

Submitted on 11 Mar 2013

HAL is a multi-disciplinary open access archive for the deposit and dissemination of scientific research documents, whether they are published or not. The documents may come from teaching and research institutions in France or abroad, or from public or private research centers.

L'archive ouverte pluridisciplinaire **HAL**, est destinée au dépôt et à la diffusion de documents scientifiques de niveau recherche, publiés ou non, émanant des établissements d'enseignement et de recherche français ou étrangers, des laboratoires publics ou privés.

IOPscience iopscience.iop.org

Home Search Collections Journals About Contact us My IOPscience

Ion diamagnetic effects in gyrofluid collisionless magnetic reconnection

This article has been downloaded from IOPscience. Please scroll down to see the full text article.

2012 J. Phys.: Conf. Ser. 401 012008

(http://iopscience.iop.org/1742-6596/401/1/012008)

View the table of contents for this issue, or go to the journal homepage for more

Download details:
IP Address: 139.124.7.126
The article was downloaded on 03/12/2012 at 15:03

Please note that terms and conditions apply.

Ion diamagnetic effects in gyrofluid collisionless magnetic reconnection

D Grasso[1], F L Waelbroeck[2], E Tassi[3],

[1]CNR-ISC, Dipartimento di Energia, Politecnico di Torino, Corso Duca degli Abruzzi, 24, 10129, Torino, Italy
[2]Institute for Fusion Studies, The University of Texas at Austin, Austin, TX 78712-1060, USA
[3]Centre de Physique Théorique, CNRS – Aix-Marseille Universités, Campus de Luminy, case 907, F-13288 Marseille cedex 09, France

E-mail: daniela.grasso@infm.polito.it

Abstract. Ion diamagnetic effects on collisionless magnetic reconnection are investigated by means of numerical simulations of a Hamiltonian gyrofluid model. The work is focused in particular on the effects of inhomogeneous density equilibria in the large Δ' regime. The linear growth rates predicted by asymptotic theory are recovered. Nonlinearly the island shape is strongly modified and the flow changes its typical four-cell structure into a simpler two cell one. Contrary to the resistive reconnection process, we find that in Hamiltonian (i.e. collisionless) reconnection the width of the final saturated island is independent from the diamagnetic effects and the magnetic island grows up to the equilibrium scale length.

1. Introduction

Due to its implication in many physical phenomena ranging from auroras in astrophysical plasmas to sawtooth crashes in Tokamak plasma [1, 2, 3], magnetic reconnection is widely studied in many different regimes and, consequently, with many different approaches. Here we are interested in high temperature and low β plasmas dominated by a strong guide field, characteristic of the Tokamak configuration. The high temperatures that characterize plasma close to ignition lead us to focus on the collisionless regime for the reconnection process, in which the electron inertia is the dominant mechanism for the decoupling between the plasma and the magnetic field motion. In the collisionless regime one of the main features of the reconnection process is the formation of narrow layers, whose width is well below the ion Larmor radius scale [4, 5]. This aspect raises also the question of which is the more appropriate physical description to be adopted. Here, as a compromise between the gyrokinetic description, accurate but computationally costly, and the fluid description that neglects all the sub-Larmor radius dynamics, we adopt the gyrofluid model described in [6]. In this framework we are interested in analyzing diamagnetic effects, generated by equilibrium ion pressure gradients, on the magnetic island evolution. In particular, among such diamagnetic effects, we focus on the island rotation and on the stabilization of the dominant mode when the diamagnetic frequency exceeds the linear growth rate [7, 8]. Moreover, we address the problem of nonlinear saturation, which results in an incomplete reconnection process and, hence, a saturated island. Indeed, one of the issues in sawtooth crashes is why the reconnection process ends before the sawtooth crash, as for instance shown in the ASDEX experiment [9]. A number of numerical simulations of the internal

kink mode and sawtooth oscillations, with various degrees of sophistication, physical models and simplifying assumptions, have also been conducted in order to interpret the experimentally observed sawtooth dynamics. [10, 11, 12, 13]. While electron inertia is always invoked to account for the fast reconnection process at the start of the sawtooth crash, the possibility to reach a saturated island has been explored in connection with different effects.
Island saturation was observed in numerical simulations in the resistive regime in Ref. [11], where a relation between the island width and the diamagnetic frequency was found following a quasi-linear approach. While in the collisionless regime a rapid rotation of the plasma core itself was shown to be responsible for incomplete reconnection whenever the equilibrium profile of the plasma pressure is sufficiently steep Ref. [12]. Here we find that the final saturated island is independent from the diamagnetic effects and the magnetic island grows up to the equilibrium scale length. Unlike [8], in this paper we focus mainly on the ion dynamics and we neglect the electron temperature effects.
The paper is organized as follows. In Sec. 2 we review the model equations. Sec. 3 compares the ion density gradient and gyroradius effects on the stability and rotation frequency of the linear dominant mode with theoretical predictions. In Sec. 4 the nonlinear phase is analyzed. We conclude in Sec. 5.

2. The model

We consider the two-dimensional version of the Hamiltonian gyrofluid model described in Ref.[6] and adopted also in Ref.[8]. The model equations are

$$\frac{\partial n_i}{\partial t} + [\Phi, n_i] = 0, \tag{1}$$

$$\frac{\partial n_e}{\partial t} + [\phi, n_e] - [\psi, \nabla^2\psi] = 0, \tag{2}$$

$$\frac{\partial}{\partial t}(\psi - d_e^2\nabla^2\psi) + [\phi, \psi - d_e^2\nabla^2\psi] + \rho_s^2[\psi, n_e] = 0, \tag{3}$$

$$n_e = \Gamma_0^{1/2} n_i + (\Gamma_0 - 1)\phi/\rho_i^2. \tag{4}$$

The first two equations represent the continuity equations for the ion guiding centers and the electrons respectively. The third equation is the Ohm's law. The system is closed by the quasi-neutrality relation (4). In Eqs.(1)-(4) n_i is the ion guiding center density, n_e the electron density, ϕ the electrostatic potential, ψ the poloidal magnetic flux function, d_e the electron skin depth, ρ_s the sonic Larmor radius and $\Phi = \Gamma_0^{1/2}\phi$ is the gyro-averaged electrostatic potential. For our analysis the Padé approximant version $\Gamma_0^{1/2} = (1 - \rho_i^2\nabla^2/2)^{-1}$ of the gyro-average operator will be adopted, where ρ_i is the ion Larmor radius. Given a Cartesian coordinate system (x, y, z), we assume all the fields be translationally invariant along z and we define the canonical bracket between two generic fields f and g by $[f, g] = \hat{z}\cdot\nabla f\times\nabla g$. Eqs. (1-4)are normalized respect to the Alfvén time and to a magnetic equilibrium scale length L. Dependent variables are normalized in the following way:

$$n_i = \frac{L}{\hat{d}_i}\frac{\hat{n}_i}{n_0}, \qquad n_e = \frac{L}{\hat{d}_i}\frac{\hat{n}_e}{n_0}, \qquad \psi = \frac{\hat{A}_z}{BL}, \qquad \phi = \frac{\hat{\rho}_s^2}{L^2}\frac{L}{\hat{d}_i}\frac{e\hat{\phi}}{T_e},$$

where carets denote dimensional variables, d_i is the ion skin depth, n_0 a background density amplitude, A_z the magnetic potential, e the unit charge, B a characteristic toroidal magnetic field amplitude and T_e the electron temperature, which is assumed to be constant.

3. Growth rate and rotation frequency in the linear phase

The model equations are solved over the domain $\{(x, y) : -\pi \leq x < \pi, -a\pi \leq y < a\pi\}$, where we prescribe the value of the number a at each simulation. The grid is composed by 1024×128 points and double periodic boundary conditions are imposed on the field perturbations, which are the quantities that the code advances in time according to a third order Adams-Bashfort scheme. The equilibrium configuration is specified by the following expressions:

$$n_{i_{eq}}(x) = n_0' x, \qquad n_{e_{eq}}(x) = n_0' x, \qquad \psi_{eq}(x) = \sum_{n=-11}^{11} a_n \exp(inx), \tag{5}$$

where n_0' is a constant and the a_n are the Fourier coefficients of the function $f(x) = A/\cosh^2 x$, where A is a parameter determining how strong is the guide field respect to the poloidal magnetic field.

The equilibrium (5) is perturbed in n_i with a four-cell pattern disturbance of the form $\tilde{n}_i \propto \cos(x + y/a) - \cos(x - y/a)$. The field ϕ is also perturbed according to (4), in such a way that the initial perturbation on n_e is zero.

Linearly we assume the fields, ψ, ϕ, n_e and n_i to behave as $\mathrm{f}(x)\exp(iky + \lambda t)$, where $\mathrm{f}(x)$ is the amplitude of the perturbation, $k = 1/a$ the wave vector, and $\lambda = \gamma + i\omega$ (here we adopt a different sign convention respect to Ref. [8]). The growth rate, γ, and the rotation frequency, ω, then correspond to the real and imaginary part, respectively, of the complex frequency λ. The set of equations, once linearized, yield the definitions: $\omega_{*e} = kn_0'\rho_s^2$ and $\omega_{*i} = -\omega_{*e}\rho_i^2/\rho_s^2$.

In Ref. [8] we presented linear results including both ion and electron diamagnetic effects, while in this paper we focus only on the ion effects. Hence, we set ρ_s and ω_{*e} to 0 and only the ρ_i scale length will be retained in our set of equations. The linear theory in Ref. [7] gives a dispersion relation (see eq. (9) in Ref. [7]), valid in the asymptotic limit $\rho_i \gg d_e$ and $\Delta' d_e >> (d_e/\rho_i)^{1/3}$, where Δ' is the standard tearing stability parameter [14]. This relation, once split into its real and imaginary part, gives the rotation frequency and the growth rate for the dominant mode according to:

$$\gamma^2 \approx \gamma_0^2 - \left(\frac{\omega_{*i}}{2}\right)^2, \tag{6}$$

$$\omega \approx \frac{\omega_{*i}}{2}, \tag{7}$$

where $\gamma_0 = 2k_y(2d_e\rho_i^2/\pi)^{1/3}$. In Fig. 1 the numerical growth rates and the rotation frequencies are plotted versus their analytical values for a simulation campaign carried out adopting $A = 1$, $a = 2$, (yielding $\Delta' = 59.9$), $d_e = 0.1$, $\rho_i = 0.2$ and n_0 ranging in the interval [0,11], which corresponds to $-0.24 < \omega_{*i} < 0$. We can see that, while for moderate values of ω_{*i} the difference between analytical and numerical values remains constant, close to the region of marginal stability such difference increases. In particular numerical simulations indicate that the stabilization is reached with a value of ion diamagnetic frequency smaller than that predicted by the theory. We remark, however, that relations (6) and (7) are valid in an asymptotic regime, and for the choice of parameters corresponding to Fig. 1, we had ρ_i only slightly grater than d_e, and $\Delta' d_e$ exceeding only five times the value of $(d_e/\rho_i)^{1/3}$. Since diminishing d_e is computationally costly, we increased the box size to better satisfy the asymptotic conditions. In Fig. 2 we show the results reporting data from a simulation campaign with $A = 1$, $a = 4$, which corresponds to $\Delta' = 240.1$, $d_e = 0.15$, $\rho_i = 0.25$ and same values of n_0 corresponding now to values of ω_{*i} in the range [-0.172,0]. For these runs $\Delta' d_e$ is 40 times the value of $(d_e/\rho_i)^{1/3}$, and the agreement with the analytical theory is considerably improved also when approaching marginal stability.

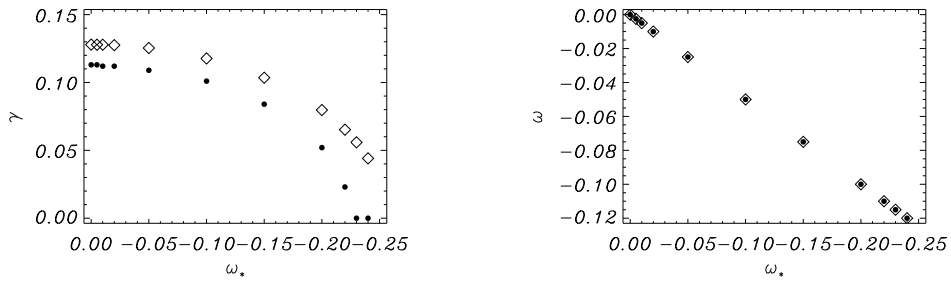

Figure 1. Comparison between the growth rates (right panel) and the rotation frequencies (left panel) obtained from the numerical simulations (circles) and the analytical values (diamonds) obtained from eqs. (6) and (7). The simulations have been carried out assuming $A = 1$, $a = 2$, $d_e = 0.1$, $\rho_i = 0.2$ and n_0' ranging from 0 to 11.

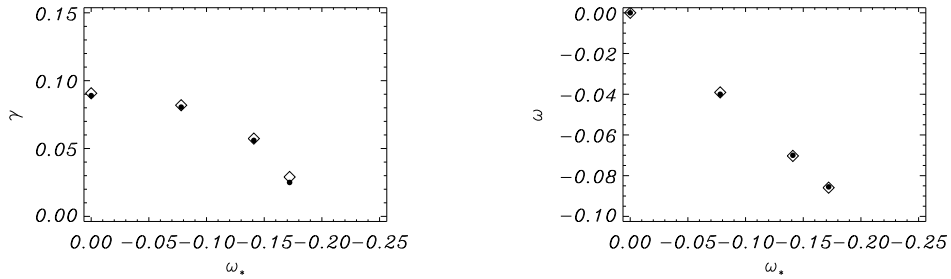

Figure 2. Comparison between the growth rates (right panel) and the rotation frequencies (left panel) obtained from the numerical simulations (circles) and the analytical values (diamonds) obtained from eqs. (6) and (7). The simulations have been carried out assuming $A = 1$, $a = 4$, $d_e = 0.15$, $\rho_i = 0.25$ and n_0' ranging from 0 to 11.

4. Nonlinear evolution

Saturation of the magnetic island induced by diamagnetic effects has been found in the resistive regime by Biskamp [11], where, following a quasi-linear approach, the island width is found to saturate at small amplitudes depending on the values of the diamagnetic frequency ω_{*i} and of the resistivity parameter η. In Ref. [12] the authors show that in the collisionless regime a partial reconnection process with island width larger with respect to the one determined in Ref. [11], is possible provided the value of the poloidal β parameter is large enough and the diamagnetic frequency is larger than the nonlinear growth rate. In this section we analyze the long term evolution of the reconnection process in order to investigate the possibility to reach a finite amplitude saturated island width resulting in partial reconnection of the plasma core. In our simulation we always find that the reconnection process evolves until the magnetic island is of the order of the equilibrium magnetic field scale length and proceeds up to the integration domain. So, no evidence of a partial reconnection process is found.

We believe that this difference is due to the intrinsic quasi-explosive behavior of magnetic

reconnection in the collisionless regime, first identified in Ref. [4]. In this regime, a typical feature is that after the linear phase the growth rate accelerates in such a way that the magnetic island reaches a macroscopic amplitude on a time that is of the order of the inverse linear growth rate [15]. In Fig. 3 the growth rates for a collisionless and a resistive case are compared. The two runs have been performed in order to have similar linear growth rate, replacing the electron inertia into the Ohm's law with a value of resistivity such that $\eta \approx \gamma d_e^2$. From this figure it is clear that while the collisionless case has a growth rate which increases after the linear phase, the resistive case goes smoothly towards saturation. In this respect, we are not in contradiction with Ref. [12]. Rather, we observe that the condition that ω_{*i} is greater than the maximum growth rate attained in the nonlinear phase, prescribed in Ref. [12] is only feebly satisfied for our parameters.

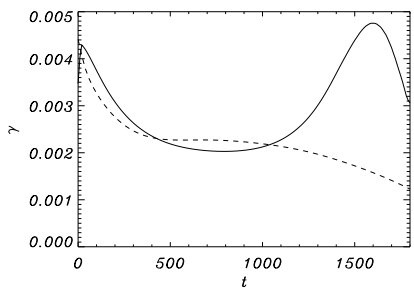

Figure 3. Comparison between the growth rate of a collisionless (solid line) and a resistive case (dashed line) having approximately the same linear growth rate. The collisionless case has a quasi-explosive behavior right after the linear phase. The simulations have been carried out setting $A = 0.03$, $a = 2$, $\rho_i = 0.2$, $n_0' = 0.4$, $d_e = 0.15$ for the collisionless case and $\eta = 0.0001$ for the resistive case.

The nonlinear evolution of the reconnection process is described in Fig. 4, where the stream function ϕ for three different values of ω_{*i} are shown. Superimposed to the plasma flow are the contour lines of the magnetic flux. For each run we have chosen to show a time step well into the nonlinear phase right after the maximum growth rate has been reached. From Fig. 3, besides

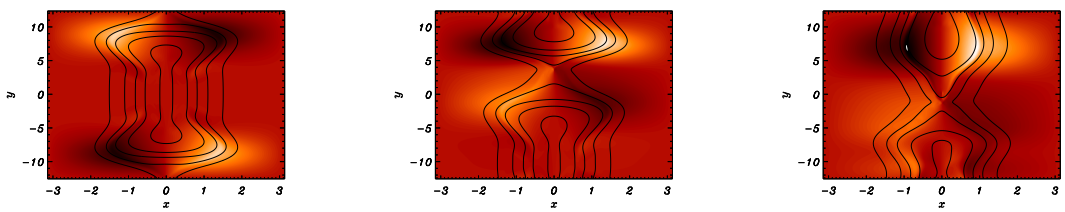

Figure 4. Comparison between the plasma flow at three different values of the diamagnetic frequency. From the left to the right $\omega_{*i} = 0, -0.078, -0.172$, corresponding to $n_0' = 0, 5, 11$ respectively. The simulations have been carried out assuming $a = 4$, $d_e = 0.15$, $\rho_i = 0.25$.

observing that the magnetic island has reached a macroscopic amplitude comparable with the scale length of the equilibrium magnetic field, we can also appreciate two different aspects of the reconnection process in this regime. First of all we observe that there is a strong nonlinear modification of the equilibrium magnetic field, due to the growth of the $k_y = 0$ wave number. Second, the plasma flow changes its structure from the typical four-cell one at $\omega_{*i} = 0$ into a two-cell one when increasing ω_{*i}. There is a progressive loss of symmetry in the y-direction related to the increasing value of the ion density equilibrium gradient.

5. Conclusions

We have investigated numerically a gyrofluid model for magnetic reconnection in collisionless regimes including ion diamagnetic effects. According to the linear theory of Ref. [7], we find stabilization for sufficiently high values of ω_{*i} and a propagation of the magnetic island in the ion direction drift. The agreement with the linear theory improves providing the asymptotic conditions for which the theory is valid are adequately satisfied. In contrast to the work presented in Ref. [8], here we focused on the difference between the saturation mechanism in the resistive regime considered in Ref. [11] and in the collisionless regime. We find that while in the resistive regime it is possible to achieve a saturated state, characterized by a finite island amplitude, corresponding to a partial reconnection process, in the collisionless regime, the magnetic island can grow up to the magnetic flux equilibrium scale length and to the integration domain, corresponding to a full reconnection process. Nonlinearly, the flow changes its topology from a symmetric four-cell structure into an asymmetric two-cell structure, when increasing the ion density equilibrium gradient.

Acknowledgments

This work was supported by the European Community under the contracts of Association between EURATOM and ENEA and between EURATOM, CEA, and the French Research Federation for fusion studies. The views and opinions expressed herein do not necessarily reflect those of the European Commission. ET acknowledges financial support from the Agence Nationale de la Recherche (ANR GYPSI)

References

[1] Priest E R and Forbes T G 2000 *Magnetic Reconnection* (Cambridge, Cambridge University Press)
[2] Biskamp D 2000 *Magnetic Reconnection in Plasmas* (Cambridge, Cambridge University Press)
[3] Wesson J A 1986 *Plasma Phys. Control. Fusion* **28** 243–248
[4] Ottaviani M and Porcelli F 1993 *Phys. Rev. Lett.* **71** 3802–3805
[5] Grasso D, Califano F, Pegoraro F and Porcelli F 2000 *Plasma Physics Reports* **26** 512–518
[6] Waelbroeck F L, Hazeltine R D and Morrison P J 2009 *Phys. Plasmas* **16** 032109
[7] Porcelli F 1991 *Phys. Rev. Lett.* **66** 425–428
[8] Tassi E, Waelbroeck F L and Grasso D 2010 *Journal of Phys. Conf. Series* **260** 012020
[9] Letsch A, Zohm H, Ryter F, Suttrop W, Gude A, Porcelli F, Angioni C and Furno I 2002 *Nuclear Fusion* **9** 1055–1059
[10] Aydemir A Y 1992 *Physics of Fluids B* **4** 3469
[11] Biskamp D 1981 *Phys. Rev. Lett.* **46** 1522–1525
[12] Biskamp D and Sato T 1997 *Phys. Plasmas* **4** 1326–1329
[13] Rogers B and Zakharov L 1996 *Phys. Plasmas* **3** 2411–2422
[14] Furth H P, Killeen L and Rosenbluth M N 1963 **6** *Physics of Fluids* 459
[15] Porcelli F, Borgogno D, Califano F, Grasso D, Ottaviani M and Pegoraro F 2002 *Plasma Physics and Controlled Fusion* **44** B389